The Effect of Knee Model on Estimates of Muscle and Joint Forces in Recumbent Pedaling

Michael J. Koehle
Biomedical Engineering Program

M. L. Hull[1]
e-mail: mlhull@ucdavis.edu

Biomedical Engineering Program and Department of Mechanical Engineering,
University of California,
Davis, CA 95616

The usefulness of forward dynamic simulations to studies of human motion is well known. Although the musculoskeletal models used in these studies are generic, the modeling of specific components, such as the knee joint, may vary. Our two objectives were (1) to investigate the effects of three commonly used knee models on forward dynamic simulation results, and (2) to study the sensitivity of simulation results to variations in kinematics for the most commonly used knee model. To satisfy the first objective, three different tibiofemoral models were incorporated into an existing forward dynamic simulation of recumbent pedaling, and the resulting kinematics, pedal forces, muscle forces, and joint reaction forces were compared. Two of these models replicated the rolling and sliding motion of the tibia on the femur, while the third was a simple pin joint. To satisfy the second objective, variations in the most widely used of the three knee models were created by adjusting the experimental data used in the development of this model. These variations were incorporated into the pedaling simulation, and the resulting data were compared with the unaltered model. Differences between the two rolling-sliding models were smaller than differences between the pin-joint model and the rolling-sliding models. Joint reactions forces, particularly at the knee, were highly sensitive to changes in knee joint model kinematics, as high as 61% root mean squared difference, normalized by the corresponding peak force of the unaltered reference model. Muscle forces were also sensitive, as high as 30% root mean squared difference. Muscle excitations were less sensitive. The observed changes in muscle force and joint reaction forces were caused primarily by changes in the moment arms and musculotendon lengths of the quadriceps. Although some level of inaccuracy in the knee model may be acceptable for calculations of muscle excitation timing, a representative model of knee kinematics is necessary for accurate calculation of muscle and joint reaction forces. [DOI: 10.1115/1.3148192]

Keywords: pedaling, recumbent, knee, simulation, subject-specific, tibiofemoral, joint reaction force, excitation, muscle, pedal force, joint angle, sensitivity

1 Introduction

Forward dynamic simulations are useful in a variety of applications, which include the study and treatment of joint disorders [1–3], sports equipment and prosthetic design [4–6], human coordination [7–9], the design of functional electrical stimulations [10,11], the optimization of sports technique, and surgical planning [12,13]. Although the musculoskeletal models used in these applications are generic, the modeling of specific components may vary.

For example, several different models exist to describe tibiofemoral kinematics. In a single degree-of-freedom model developed by Yamaguchi and Zajac [14], the position of the femur relative to the tibia is defined by the flexion angle and two coupled translations in the sagittal plane. These translations follow prescribed functions of the flexion angle inferred from the geometry of tibiofemoral contact surfaces and tibiofemoral contact point data reported by Nisell [1]. In another single degree-of-freedom model, the functions describing the coupled translations are derived from an inextensible four-bar linkage, consisting of the anterior and posterior cruciate ligaments along with the femur [15,16]. A final model describes the tibiofemoral joint as a fixed revolute, with no coupled translations [10,17–19].

It is unknown how the tibiofemoral joint model affects the simulation results, but this effect may be substantial. The location of the knee joint center controls the lengths of the tibia and femur segments. These lengths in turn affect both the net joint moment required for a given motion, as well as the moment arms and musculotendon lengths of all muscles that span the knee joint, and so could substantially affect both the muscle forces and joint contact forces returned by the simulation. Hence one objective of this study was to analyze the effect on simulation results for each of the three knee joint models above.

Forward dynamic simulations often use generic musculoskeletal models, but a need for subject-specific models has been recognized. Subject-specific models would enable surgeons to plan for patient-specific surgeries and to recommend patient-specific rehabilitation strategies. Subject-specific models could also impact the design and use of prosthetics, sports equipment, and sports technique. With the development of instrumented knee and hip replacement devices [20,21], it is now possible to validate the joint contact forces predicted by a forward dynamic simulation. This validation would require a subject-specific model. Although methods of determining subject-specific model parameters have been developed [22–25], and the sensitivity of simulations to some of these parameters have been explored [19,26,27], it is largely unknown how variations in many of these model parameters affect simulation results. To determine which model parameters need to be subject-specific and the level of accuracy required for these parameters, it is necessary to know the sensitivity of a simulation to these parameters. The second objective of this study was to analyze the sensitivity of the joint contact forces and

[1]Corresponding author.

Contributed by the Bioengineering Division of ASME for publication in the JOURNAL OF BIOMECHANICAL ENGINEERING. Manuscript received November 28, 2007; final manuscript received March 3, 2009; published online December 17, 2009. Review conducted by Jennifer S. Wayne.

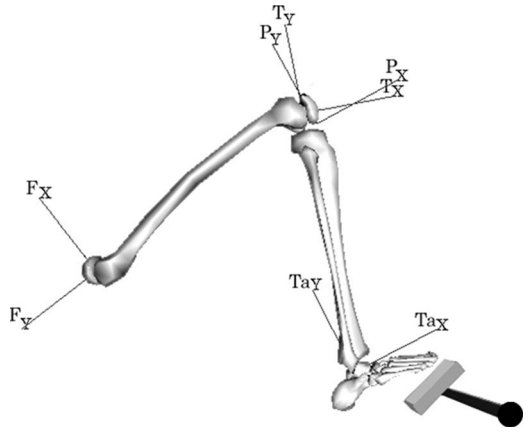

Fig. 1 The right leg of the pedaling model. Coordinate systems are shown for the femur (F), tibia (T), patella (P), and talus (Ta) segments.

muscle forces returned by a forward dynamic simulation to realistic variations in knee kinematics for the knee model by Yamaguchi and Zajac [14], which is the most commonly used of the three knee models above.

2 Methods

A two-dimensional forward dynamic simulation of pedaling was used to study the effect of knee joint models and variations in kinematics on simulation results. The musculoskeletal model was adapted from an upright pedaling model [28,29] to recumbent pedaling [30]. The skeletal model consisted of nine segments: a pelvis and left and right femur, tibia, patella, and foot segments (Fig. 1). Each foot was fixed rigidly to a pedal, which was connected to the crank through a simple revolute joint. The pelvis was fixed in space. Both the hip and ankle joints were modeled as revolutes. The knee joint was modeled in several different ways to be described later. The skeletal model was driven by 78 Hill-type muscle-tendon actuators, a subset of those used in a walking model [31]. Crankload dynamics were modeled by applying an equivalent inertial and resistive torque about the center of crank arm rotation [32].

Equations of motion for the pedaling model were generated using SD/FAST (Symbolic Dynamics, Mountain View, CA). A forward dynamic simulation was produced using SIMM in conjunction with dynamics pipeline (MusculoGraphics, Evanston, IL). Muscle excitations were found using computed muscle control [33,34], which uses static optimization along with feedforward and feedback controls to reproduce or "track" essential features of the subject's experimental data. For the static optimization problem, muscle excitations were found that minimized the sum of the activations squared [35]. The experimental data to be tracked were previously obtained averaged crank and pedal angles and radial pedal forces, collected from 15 male cyclists, ranging from 18 years to 60 years, pedaling at a rate of 90 rpm and a workrate of 250 W [36]. Thelen et al. [33] demonstrated that tracking these quantities was sufficient to reproduce experimental kinematics and electromyogram (EMG) timing. It is not necessary to track tangential pedal forces because they are directly related to crank accelerations.

The knee joint reaction forces computed by SIMM were further processed according to a method detailed elsewhere [37], but described briefly here. The SIMM knee model defines a joint between the patella and tibia so that patellotibial kinematics can be prescribed. No force is transmitted through the patellar ligament, which is not modeled. Hence the knee joint reaction forces computed by SIMM are not physiologic—the tibiofemoral joint reaction force could be primarily shear with the knee flexed, and a patellofemoral joint reaction force is not calculated. To calculate physiologic patellofemoral and tibiofemoral joint reaction forces, the fictional patellotibial joint reaction force was removed, and a force was applied through the patellar ligament. The magnitude of this force was found so that the resulting moment about the tibiofemoral instantaneous joint center was equal to the moment resulting from the quadriceps muscles. The resulting contribution of the quadriceps to the tibiofemoral joint reaction force is primarily compressive, and a physiologic patellofemoral joint reaction force is calculated.

2.1 Objective 1. Three different models of the tibiofemoral joint were incorporated into the pedaling simulation. In two of these models, translations of the knee joint center in the sagittal plane were coupled to knee flexion angle, but differed in the functions used to describe the coupled motions. In the third model, the tibiofemoral joint was a simple pin joint, with a stationary knee joint center.

The first model, hereafter referred to as the contact model, was that developed by Yamaguchi and Zajac [14] and modified by Delp et al. [38]. Using a combination of bone geometry and the experimental tibiofemoral contact pathway data reported by Nisell [1], Yamaguchi et al. extrapolated the orientation of the femur relative to the tibia. In this model, the tibiofemoral contact surface of the femur in the sagittal plane was represented by an ellipse. The contact surface of the tibia was approximated by a straight line, offset from the tibial anterior-posterior axis. The position of the tibia relative to the femur at each degree of flexion was found by constraining the tibiofemoral contact point to follow the path along the tibial plateau reported by Nisell. Nisell defined the contact point as the midpoint on the shortest distance between the femur and tibia. This point was found from lateral radiographs of 20 subjects standing at various knee flexion angles.

In a second model, the kinematics of the tibiofemoral joint were developed using an inextensible four-bar linkage, consisting of the anterior cruciate ligament (ACL), posterior cruciate ligament (PCL), the tibia, and the femur [16,39]. Parameters describing ligament attachment locations were based on the measurements of van Dijk et al. [40], and parameters describing bone dimensions were based on anatomical measurements [39,41]. As with the contact model, the tibial contact surface was approximated by a straight line, but normal to the tibial proximal-distal axis. The femoral condyle was approximated by a circle. The point where the ligaments crossed was defined as the instant center of zero velocity of either body relative to the other. To avoid either separation or penetration at the contact surface between the tibia and femur, the line normal to both articular surfaces at the contact point must pass through this instant center. Although the radius and location of the circle representing the condyle are not explicitly stated in the literature related to the model, they were found by choosing a radius and location that minimizes the square of the distance between the contact point and the most distal point of the circle. Because the four-bar linkage has only one degree of freedom, the pose of the femur relative to the tibia depends on the flexion angle. With knowledge of the location of the femur origin relative to the ACL and PCL ligament attachments sites, translations describing the position of the tibia relative to the femur as a function of flexion angle were found.

Finally, in the pin-joint model, the flexion axis of the simple revolute was coincident with the epicondylar axis (Fig. 2). This axis has been shown to correspond closely with the functional flexion-extension axis [42]. Although this knee model does not attempt to emulate the rolling motion observable in real knees, it is still often employed in musculoskeletal models [10,17–19].

Each tibiofemoral model was incorporated into the existing musculoskeletal model. The four-bar linkage was scaled homogeneously so that the anterior-posterior depth of the femur was equal to that of the contact model. The depth of the femur has been shown to provide good correlation with many other knee parameters [43]. In the contact model, this depth was given by the el-

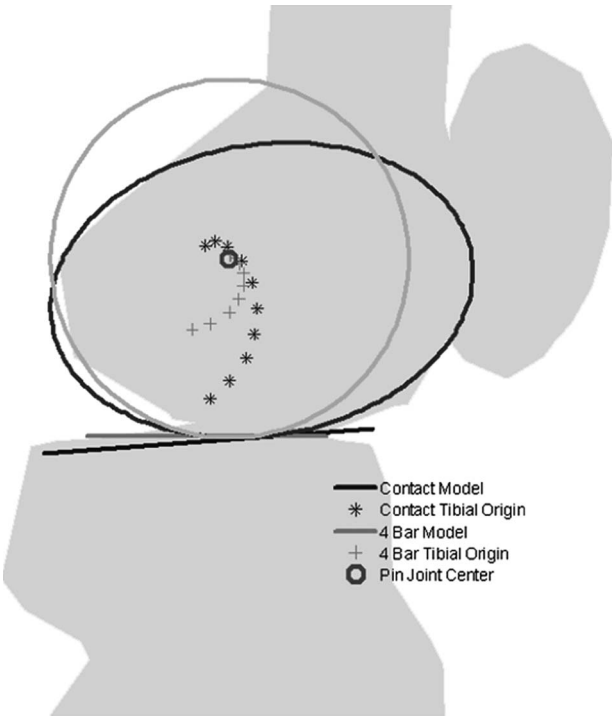

Fig. 2 The contact, four-bar, and pin-joint models. The origins are shown relative to the femur for different angles of flexion, ranging from 0 deg to 120 deg in 10 deg increments.

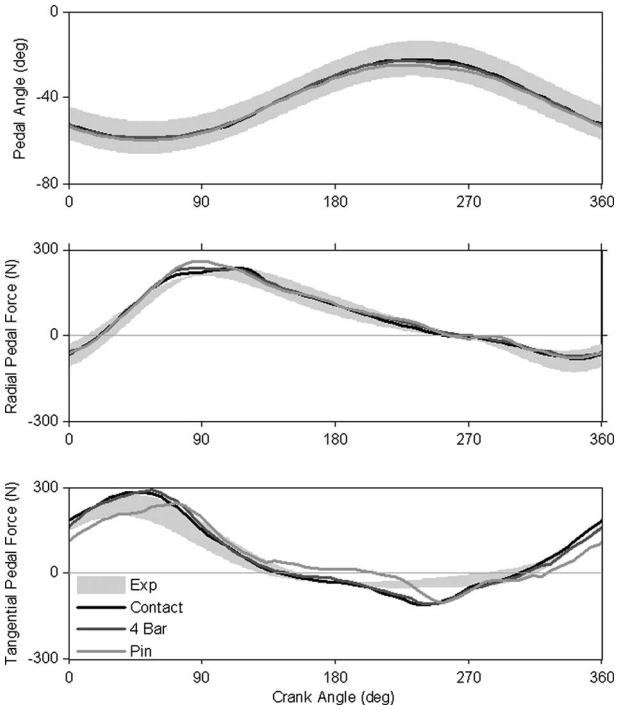

Fig. 3 Simulation results for the three knee models and experimental results. The gray area is the experimental data +/−1 standard deviation. At 0 deg crank angle, the crank arm is vertical. Positive radial force is toward the crank axis. Positive tangential force is forward.

lipse representing the femoral condyles. In the four-bar linkage model, the depth was the sum of two circles, and the offset between them. The patellotibial kinematics of each knee model were based on the model developed by Delp et al. [38], which was used with all three tibiofemoral models. No other model parameters were changed.

Normalized root mean squared (rms) differences were used to analyze the sensitivity of the simulations to the various knee models. Root mean squared differences for generated pedal angle, radial pedal force, and tangential pedal force data were calculated with respect to experimental averages. Root mean squared difference for pedal angle were normalized by the range of experimental pedal angles. The radial and tangential pedal force components were normalized by the corresponding maximum absolute experimental force. For data for which there were no experimental measures—joint reaction forces, muscle forces, and muscle excitations—rms differences for the four-bar and pin-joint models were calculated with respect to the contact model. Joint reaction force components were normalized by the contact model's corresponding maximum absolute force. Joint reaction forces were inclusive of both bone-on-bone contact forces and unmodeled soft tissue forces. Muscle forces were normalized by the contact model's corresponding maximum force for that muscle. By definition, muscle excitations ranged from 0 to 1, and so were not normalized. Differences were calculated as a function of crank angle. Cubic splines were fit to each data set so that differences could be taken at identical crank angles.

2.2 Objective 2. Beginning with its incorporation into the musculoskeletal model developed by Delp et al. [38], the contact model is arguably the most commonly used knee model in forward dynamic simulations of human motion. For this reason, this model was used in the sensitivity analysis of knee joint contact forces and muscle forces.

To vary the tibiofemoral model, it was first necessary to reproduce the original knee model. Although the knee model is described in Ref. [38], several specifics are missing including key geometric relations, such as the dimensions of the ellipse representing the contact surface, the tilt of this ellipse, and the tilt of tibial plateau. Using the contact data reported by Nisell, these relations were found that reproduced the tibiofemoral kinematics given in the SIMM joint file within a rms difference of 1 mm [44].

Variations in tibiofemoral kinematics were made by adjusting the contact pathway data according to the standard deviations reported by Nisell [1]. All contact points within a knee model variation were moved consistently either anteriorly or posteriorly along the tibial plateau a percentage of the standard deviation for a particular contact point. Within each model variation, each contact point standard deviation was scaled consistently by the same percentage. Percentages applied to each variation were spaced incrementally from two standard deviations posterior to the average to two standard deviations anterior to the average. New tibiofemoral kinematics were calculated, so that, at a specified flexion angle, the elliptical representation of the femoral condyles came in contact with the tibial plateau at the point specified by the new contact pathway [14,38]. At two deviations posterior, the rms difference in the origin of tibia in the femoral coordinate system with respect to the reference model was 7.9 mm. At two deviations anterior, the rms difference was also 7.9 mm. Root mean squared differences increased linearly with the magnitude of the deviation.

The patellotibial model employed in the sensitivity analysis used experimental measures of patellar and patellar ligament rotation relative to the tibia to define patellotibial kinematics [38]. These rotations were determined from lateral radiographs of cadaveric knees at various angles of knee flexion [45]. The length of patellar ligament was assumed constant. The insertion point of the patellar ligament used in this model was not found in the literature, so the insertion point that best reproduced the kinematics recorded in the original SIMM joint file was used [44].

Patellotibial kinematics were varied by adjusting the patellar ligament rotation angle, according to the standard deviations given by van Eijden et al. [45]. The same percentage of the standard deviation was used to adjust the patellar ligament angle

Table 1 Normalized rms differences calculated for the three knee models. Normalized rms differences for tracking results are computed with respect to average experimental data. All other differences are computed with respect to the contact knee model. Hip, tibiofemoral, patellofemoral, and ankle joint reaction forces are given, respectively, in the femur, tibia, patella, and talus coordinate systems (Fig. 1). Pedal forces were normalized by the maximum absolute experimental values. Pedal angles were normalized by the range of experimental pedal angles. Muscle force and joint reaction forces were normalized by the contact model's corresponding maximum absolute value. Muscles were abbreviated as follows: GMAX =gluteus maximus, GMED=gluteus medius, IL=iliacus, VASL =vastus lateralis, BFLH=biceps femoris (long head), SEMT =semitendinosus, BFSH=biceps femoris (short head), TA =tibialis anterior, MGAS=medial gastrocnemius, SOL=soleus.

	Contact (%)	Four-bar (%)	Pin (%)	100%=
	Tracking			
Pedal angle	1.2	1.5	4.9	37 deg
Radial pedal force	5.4	7.2	8.9	219 N
Tangential pedal force	13.8	14.1	16.7	236 N
	Excitations			
GMAX		5.1	10.7	
GMED		12.2	16.9	
IL		13.0	18.0	
VASL		7.9	14.2	
BFLH		6.4	15.6	
SEMT		9.7	20.0	
BFSH		8.9	16.0	
TA		2.9	5.2	
MGAS		6.9	7.3	
SOL		3.3	6.4	
	Muscle forces			
GMAX		4.0	12.0	179 N
GMED		15.2	19.9	326 N
IL		8.0	15.3	565 N
VASL		14.9	29.7	548 N
BFLH		6.5	33.0	211 N
SEMT		12.3	32.1	164 N
BFSH		10.7	18.0	339 N
TA		18.8	24.9	102 N
MGAS		9.6	12.2	185 N
SOL		7.5	15.8	389 N
	Joint forces *x*-component			
Hip		13.5	22.7	961 N
Knee (tibiofemoral)		11.3	22.6	809 N
Knee (patellofemoral)		18.9	35.6	1425 N
Ankle		6.7	13	290 N
	y-component			
Hip		3.5	11.7	2141 N
Knee (tibiofemoral)		11.9	22.3	1441 N
Knee (patellofemoral)		27.2	22.5	833 N
Ankle		3.7	10.3	1075 N

within each model variation. These percentages were spaced incrementally from positive two standard deviations to negative two standard deviations. Using the adjusted patella rotation angles, new patellotibial kinematics were calculated. At two standard deviations posterior, the rms difference in the origin of patella in the tibial coordinate system with respect to the reference model was 10.8 mm. At two standard deviations anterior, the rms difference was also 10.8 mm. Root mean squared differences increased linearly with the magnitude of the deviation.

For each tibiofemoral and patellotibial model variation, computed muscle control was used to compute muscle excitations. Model comparisons were made on the basis of rms differences, as

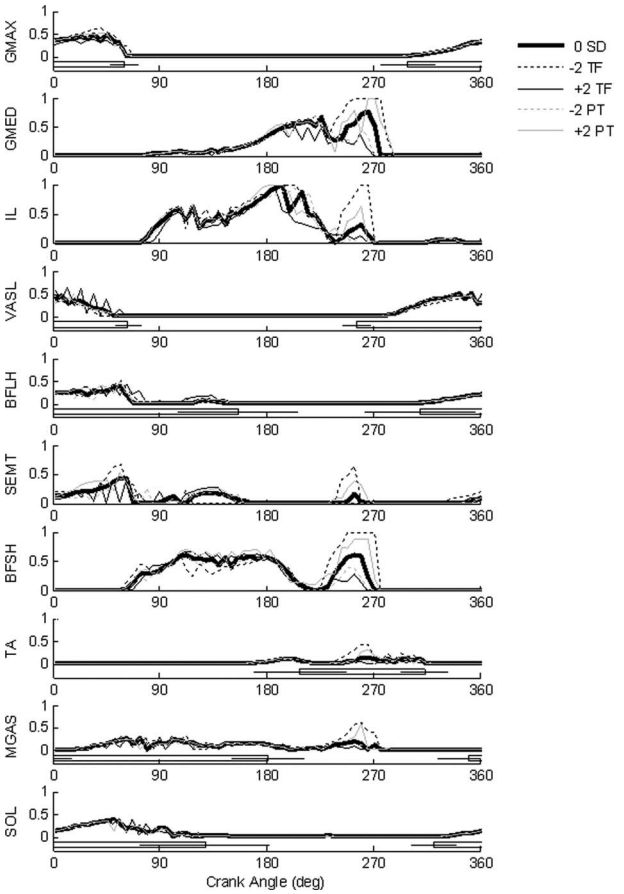

Fig. 4 Muscle excitations generated from computed muscle control for variations in the kinematics of the patellotibial (PT) and patellofemoral (PF) models. −2 TF and +2 TF are the −2 standard deviation and +2 standard deviation tibiofemoral model variations, respectively. −2 PT and +2 PT are the −2 standard deviation and +2 standard deivation patellotibial model variations respectively. 0 SD is the unaltered reference model. For comparison, the experimental on-off timing of the EMG activity +/−1 standard deviation is given for muscles for which this data was available [30].

with Objective 1. For all results, including pedal angles, pedal forces, joint reaction forces, muscle forces, and muscle excitations, rms differences were calculated for each variation with respect to the reference model. In the tibiofemoral case, the reference model was the model generated using the averaged contact point data. For the patellotibial model, the reference model was the model generated using the averaged patella rotation angle.

3 Results

3.1 Objective 1. Although all three models reproduced the experimental data (pedal angle and radial and tangential pedal forces) well (Fig. 3), the contact model consistently returned the smallest differences, followed closely by the four-bar model (Table 1). For both the contact and four-bar models, pedal angles were reproduced within a normalized rms difference of 1.5%. Radial pedal forces were also well tracked to within 1 standard deviation except at around 90 deg crank angle; the normalized rms difference was 5.4%. Tangential pedal force was less well tracked with the normalized rms difference being about 2.5 times that of the radial pedal force.

For the generated muscle excitations, muscles forces, and joint reaction forces, the differences between the contact and four-bar models were usually smaller than the differences between the con-

Table 2 Normalized rms differences for tibiofemoral (TF) and patellotibial (PT) model variations relative to the reference tibiofemoral and patellotibial models respectively. For all data, rms differences increased approximately linearly with the magnitude of the variation. For this reason, only the extreme values at +/−2 standard deviations are shown

	TF, −2 (%)	TF, +2 (%)	PT, −2 (%)	PT, +2 (%)	100%=
		Tracking			
Pedal angle	1.4	1.5	0.3	0.2	37 deg
Radial pedal force	8.6	4.5	1.2	1.3	238 N
Tangential pedal force	7.0	4.3	2.4	5	283 N
		Excitations			
GMAX	5.3	5.3	2.6	2.6	
GMED	17.8	14.0	12.1	14.3	
IL	19.4	12.3	9.5	10.5	
VASL	5.3	8.4	3.5	3.1	
BFLH	3.7	7.5	3.6	3.8	
SEMT	14.1	9.2	5.5	7.2	
BFSH	20.6	10.4	8.2	13.4	
TA	7.3	3.0	2.3	3.2	
MGAS	11.8	6.7	5.1	6.4	
SOL	2.9	4.2	2.2	3.0	
		Muscle Forces			
GMAX	8.0	5.5	1.2	2.4	179 N
GMED	20.7	17.3	12.4	15.5	326 N
IL	11.0	8.3	5.1	5.7	565 N
VASL	22.0	11.9	12.7	30.3	548 N
BFLH	7.5	14.6	5.5	8.6	211 N
SEMT	39.4	12.3	10.4	21.0	164 N
BFSH	29.2	15.3	10.6	16.4	339 N
TA	55.4	19.9	13.2	21.7	102 N
MGAS	24.5	8.1	6.1	9.9	185 N
SOL	6.3	6.7	1.7	3.3	389 N
		Joint forces			
		x-component			
Hip	22.7	15.5	9.6	13.9	961 N
Knee (tibiofemoral)	32.7	13.4	39.6	13.0	809 N
Knee (patellofemoral)	18.6	9.1	29.2	32.3	1425 N
Ankle	18.1	7.0	3.6	6.3	290 N
		y-component			
Hip	9.1	4.2	2.7	5.2	2141 N
Knee (tibiofemoral)	14.9	8.7	32.6	10.9	1441 N
Knee (patellofemoral)	14.9	6.5	61.3	30.1	833 N
Ankle	13.3	4.9	2.9	5.2	1075 N

tact and pin-joint models (Table 1). Normalized rms differences for muscle forces and joint reaction forces were higher than muscle excitations. The biceps femoris (long head), vastii, and semitendinosus were most sensitive, at approximately 30% rms. Patellofemoral joint reaction forces were affected the most at 35.6% (507 N) for the *x*-component of the pin-joint model and 27.2% (227 N) for the *y*-component of the four-bar model. Tibiofemoral joint reaction forces for the pin-joint model were also strongly affected at 22% for both the *x*- and *y*-components.

3.2 Objective 2. For both tibiofemoral and patellotibial variations, differences in tracked data and muscle excitations were small relative to the differences in muscle forces and joint reaction forces. Excitation on/off timing closely matched the EMG data for all models (Fig. 4), falling within 1 standard deviation of the experimental on/off point for most muscles. Normalized rms differences for tracked data and muscle excitation were generally below 10% (Table 2). Exceptions were the excitation of the biceps femoris (short head) at 20.6%, the iliacus at 19.4%, and the gluteus medius at 17.8% all three of which occurred for the −2 standard deviation tibiofemoral model variation. Forces of several muscles were particularly sensitive midway through the second half of the crank cycle, including the vastii, biceps femoris (short head), semitendinosus, tibialis anterior, and gastrocnemius (Table 2, Fig. 5). Joint reaction forces were also sensitive, particularly at the knee, and were as high as 61.3% for patellotibial model variations and 14.9% for tibiofemoral model variations. Joint reaction forces were particularly sensitive over the second half of the crank cycle. (Fig. 6).

Root mean squared differences were generally higher for tibiofemoral variations than patellotibial variations by as much as 10%, with the exception of knee joint reaction forces (Table 2). The *y*-components of the tibiofemoral and patellofemoral joint reaction forces were higher for patellotibial model variations by 17.7% and 46.4%, respectively.

4 Discussion

Several different models exist to describe tibiofemoral kinematics, but the effect of the knee model on forward dynamic simulation results is unknown. Hence one objective of the present study was to investigate the effect of three commonly used tibiofemoral joint models on forward dynamic simulation results. Because of the need for subject-specific knee models, a second objective was to investigate the sensitivity of forward dynamic simulation results to variations in kinematics of the most widely used of the

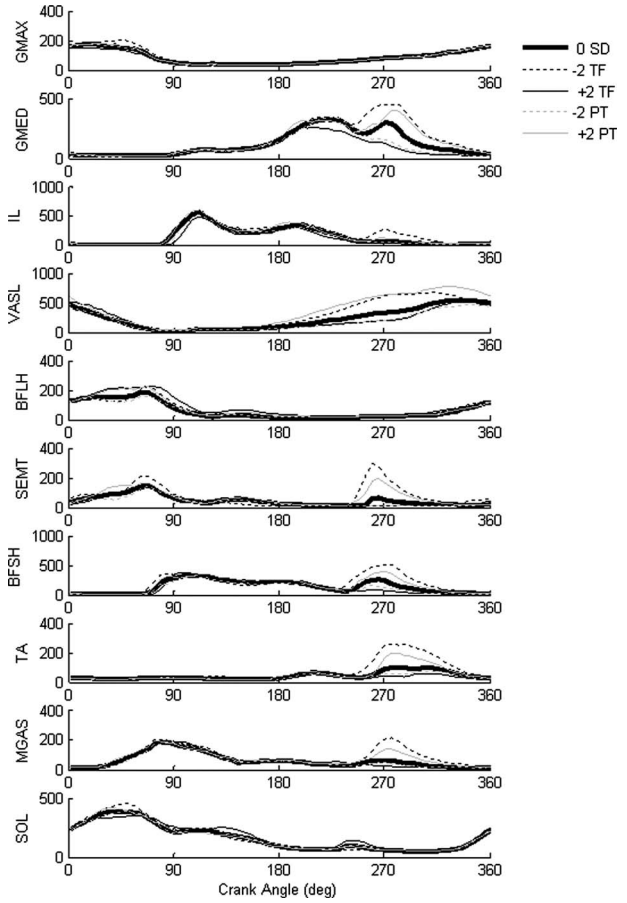

Fig. 5 Muscle forces over a complete crank cycle for the reference contact model and for variations in the kinematics of the tibiofemoral (TF) and patellotibial (PT) models. −2 TF and +2 TF are the −2 standard deviation and +2 standard deviation tibiofemoral model variations, respectively. −2 PT and +2 PT are the −2 standard deviation and +2 standard deviation patellotibial model variations, respectively. 0 SD is the unaltered reference model. Forces were sensitive to the kinematic variations over the second half of the crank cycle. Only results for extreme kinematic variations are shown. The vastus intermedius and vastus lateralis are not shown, but behaved similarly to the vastus medialis.

three knee models. Differences in the contact and four-bar models were small compared with differences between the pin-joint model and the contact model. With the exception of knee joint reaction forces, forward dynamic simulation results were more sensitive to changes in tibiofemoral kinematics than to changes in patellotibial kinematics. In general, muscle excitations, pedal angle, and pedal forces were less sensitive to changes in knee model than muscle forces and joint reaction forces, particularly at the knee.

4.1 Objective 1. From comparing simulation results for the three tibiofemoral models, we found that with regard to pedal forces, pedal angles, and muscle excitation data, the two rolling-sliding models behaved similarly. For these output quantities, differences between the pin-joint and the contact model were more pronounced, but were still generally small with respect to their normalizing values. Muscle forces and joint reaction forces, however, were affected strongly by the type of knee model. The reasons behind this sensitivity are similar to those for the high sensitivity in these same quantities to variations in knee kinematics and will be given in the discussion related to Objective 2, which follows. These results suggest that a simplified knee model may be sufficient for those applications concerned with output excitation timing, or where a certain amount of imprecision is acceptable. However, if either accurate muscle or joint reaction forces are of interest, then a more accurate knee model is required.

One limitation in comparing the simulation results for the three different knee models was that only tibiofemoral kinematics differed. The patellotibial model was designed for use with the contact model [38]. The four-bar and pin-joint models each are part of complete musculoskeletal models, with their own method of describing the patella. Simulations incorporating the pin joint often model the patella as a single wrapping point in the path of the quadriceps, which may be grouped into a single actuator [17,19]. The patellotibial kinematic model used with the four-bar tibiofemoral model required the grouping of the quadriceps muscles into a single actuator, with a single insertion and origin [46]. Furthermore, in the four-bar model, a single wrapping point was used to represent the muscle's interaction with the femur rather than a wrapping surface. Because the present study is concerned with an investigation of knee kinematics, it was undesirable to alter the muscles modeled. For this reason, only the tibiofemoral models were compared.

The areas of sensitivity in muscle excitations, muscle forces, and joint reaction forces were similar to those of Objective 2, as shown in Figs. 4–6. Hence, similar plots for Objective 1 were deemed redundant and were not included.

4.2 Objective 2. Forward dynamic simulation results were generally more sensitive to changes in tibiofemoral kinematics than to patellotibial kinematics. This was expected because variations in tibiofemoral kinematics affect the moment arms and musculotendon lengths of all muscles that cross the knee joint, whereas variations in patellotibial kinematics affect only the moment arms and musculotendon lengths of the quadriceps muscles. Muscle forces and joint reaction forces were sensitive to variations in both tibiofemoral and patellotibial kinematics.

Variations in tibiofemoral and patellofemoral kinematics could have been created using other means. For example, tibiofemoral kinematics also could have been altered by changing the dimensions of the ellipse representing the femoral condyles. Patellotibial variations also could have been created by adjusting patellar rotation angles rather than the patellar ligament rotation angles. However, because the correlations between bone geometry and contact point or patellar ligament rotation angle and patellar rotation angle were not known, only one characteristic was chosen. Although this might be an oversimplification, adjusting more than one characteristic without knowledge of how other characteristics were correlated could result in knee kinematics, which are not physiologic. Hence adjusting the contact pathway was chosen for the tibiofemoral joint model because standard deviations were readily available. Patellar ligament rotation angle was chosen for the patellotibial joint model because inconsistencies were found in the patellar rotation data, extracted from the existing knee model and the experimental data [44].

For both the contact point and patellar rotation angle inputs, all inputs within a model variation were adjusted by the same percentage of the standard deviation, rather than adjusting each data point individually. For both patellar rotation angle and contact point, individual subject data were not available so that some assumption as to how each data point was subject dependent or autocorrelated was necessary. Using a Monte Carlo simulation, where different degrees of autocorrelation were tested, it was found that assuming complete autocorrelation produced kinematic variations that were greater than those variations achieved by allowing each data point a degree of individual variation [44]. With regard to tibiofemoral kinematics, this assumption is further supported by the data reported by Montgomery et al. [47], which show that extensive autocorrelation occurs for tibiofemoral contact point.

The differences observed in muscle excitations, muscle forces, and joint reaction forces were not a result of changes in either

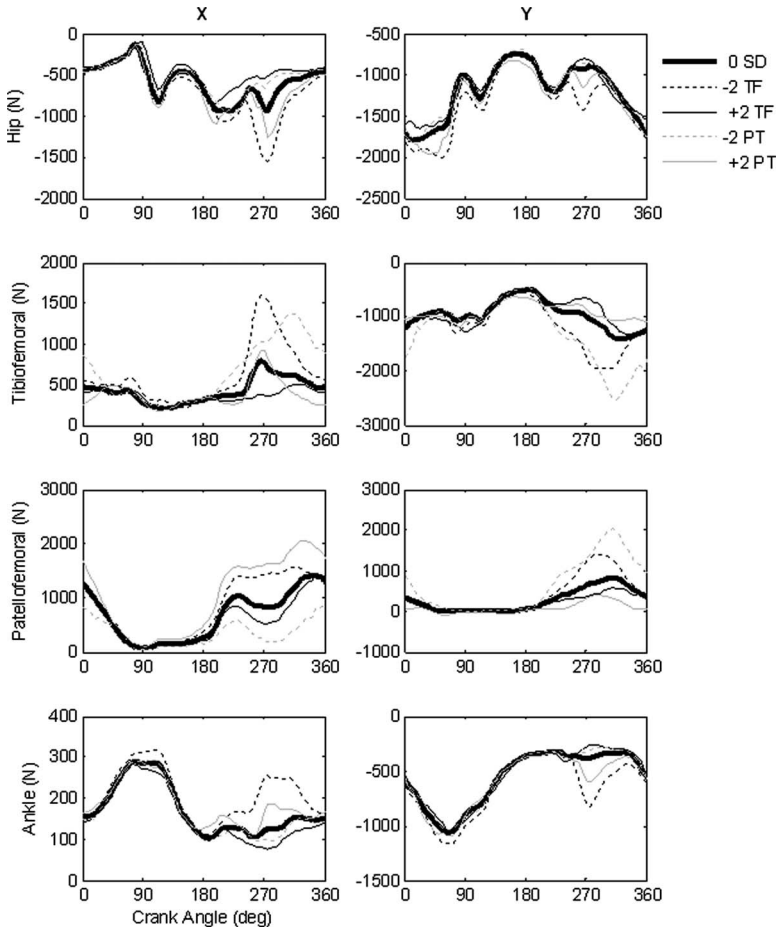

Fig. 6 Joint reaction forces over a complete crank cycle for the reference model and for variations in the kinematics of the tibiofemoral (TF) and patellotibial (PT) models. −2 TF and +2 TF are the −2 standard deviation and +2 standard deviation tibiofemoral model variations, respectively. −2 PT and +2 PT are the −2 standard deviation and +2 standard deviation patellotibial model variations, respectively. 0 SD is the unaltered reference model.

intersegmental forces or moments, which were small. Differences in intersegmental forces, which are the sum of the joint reaction forces and muscle force contribution at each joint, were below 1% rms difference for all joints, when normalized by the reference model's corresponding maximum intersegmental force. Likewise differences in intersegmental moments were small, less than 1% rms when normalized by the reference model's corresponding maximum intersegmental moment.

Changes in simulation results were caused by changes to musculotendon lengths and muscle moment arms. Although these changes were not large, less than 10% rms (normalized by the reference model's peak values), because several muscles were affected simultaneously, these changes had a marked impact on simulation results. This is illustrated in the second half of the crank cycle (Figs. 5 and 6).

The increased sensitivity over the second half of the crank cycle is primarily an effect of the changes to the quadriceps' moment arms and musculotendon lengths. At about 180 deg crank angle, the vastii generate a passive force. Changes in musculotendon length of the vastii affect the magnitude of this force. Cocontracting muscles on the opposite side of the leg must compensate to achieve the same net joint moment. For example, at the −2 standard deviation tibiofemoral model variation, the lengths of the vastii increase, leading to an increase in their passive force. At the same time, their moment arms increase, while the hamstrings moment arms decrease. To achieve the same net joint moment, the excitations of the biceps femoris (short head), medial gastrocnemius, and semitendinosus must increase dramatically (Fig. 4). At 270 deg crank cycle, the excitations of these muscles drop off, but they continue to generate a passive force (Fig. 5), requiring cocontraction by the quadriceps muscles. Because some of the muscles crossing the knee are bi-articular, the hip and ankle net joint moments are affected and must be compensated for by cocontractions in other muscles at these joints. In this manner, muscles forces on opposite sides of the leg can increase or decrease together, summing to cause large changes in the joint reaction forces.

In summary, our results show that the choice of the knee joint model affects the results of forward dynamic simulations particularly the muscle and joint reaction forces with little effect on the muscle excitations. Differences between the two rolling-sliding models were smaller than differences between the pin-joint model and the rolling-sliding models. Similarly, joint reaction forces and muscle forces were more sensitive to variations in knee model kinematics, while muscle excitations were less sensitive. Generally, tibiofemoral variations resulted in greater rms differences in results than patellotibial variations, with the exception of knee joint reaction forces, which were more sensitive to patellotibial variations. The observed sensitivity was not due to changes in either intersegmental forces or net joint moments, but was prima-

rily an effect of changes to the moment arms and musculotendon lengths of the quadriceps. Although some level of inaccuracy in the knee model may be acceptable for determining muscle excitations, a representative model of knee kinematics is necessary for the accurate calculation of muscle and joint reaction forces.

Acknowledgment

We acknowledge funding from NIDRR (Award No. H133G020137) for financial support of this project. The authors are also grateful to Dr. Darryl Thelen and David Remy for their assistance with implementing the computed muscle control algorithm.

References

[1] Nisell, R., 1985, "Mechanics of the Knee. A Study of Joint and Muscle Load With Clinical Applications," Acta Orthop. Scand. Suppl., **216**, pp. 1–42.
[2] Kuster, M. S., Wood, G. A., Stachowiak, G. W., and Gachter, A., 1997, "Joint Load Considerations in Total Knee Replacement," J. Bone Joint Surg. Br., **79**(1), pp. 109–113.
[3] Neptune, R. R., and Kautz, S. A., 2000, "Knee Joint Loading in Forward Versus Backward Pedaling: Implications for Rehabilitation Strategies," Clin. Biomech. (Bristol, Avon), **15**(7), pp. 528–535.
[4] Ekevad, M., and Lundberg, B., 1995, "Simulation of 'Smart' Pole Vaulting," J. Biomech., **28**(9), pp. 1079–1090.
[5] Kautz, S. A., and Hull, M. L., 1995, "Dynamic Optimization Analysis for Equipment Setup Problems in Endurance Cycling," J. Biomech., **28**(11), pp. 1391–1401.
[6] Jin, D., Zhang, R., Dimo, H. O., Wang, R., and Zhang, J., 2003, "Kinematic and Dynamic Performance of Prosthetic Knee Joint Using Six-Bar Mechanism," J. Rehabil. Res. Dev., **40**(1), pp. 39–48.
[7] Fregly, B. J., and Zajac, F. E., 1996, "A State-Space Analysis of Mechanical Energy Generation, Absorption, and Transfer During Pedaling," J. Biomech., **29**(1), pp. 81–90.
[8] Zajac, F. E., 2002, "Understanding Muscle Coordination of the Human Leg With Dynamical Simulations," J. Biomech., **35**(8), pp. 1011–1018.
[9] Kautz, S. A., Neptune, R. R., and Zajac, F. E., 2000, "General Coordination Principles Elucidated by Forward Dynamics: Minimum Fatigue Does Not Explain Muscle Excitation in Dynamic Tasks," Motor Control, **4**(1), pp. 75–80, discussion pp. 97–116.
[10] Gfohler, M., and Lugner, P., 2004, "Dynamic Simulation of FES-Cycling: Influence of Individual Parameters," IEEE Trans. Neural Syst. Rehabil. Eng., **12**(4), pp. 398–405.
[11] Dariush, B., Parnianpour, M., and Hemami, H., 1998, "Stability and a Control Strategy of a Multilink Musculoskeletal Model With Applications in FES," IEEE Trans. Biomed. Eng., **45**(1), pp. 3–14.
[12] Delp, S. L., Statler, K., and Carroll, N. C., 1995, "Preserving Plantar Flexion Strength After Surgical Treatment for Contracture of the Triceps Surae: A Computer Simulation Study," J. Orthop. Res., **13**(1), pp. 96–104.
[13] Riewald, S. A., and Delp, S. L., 1997, "The Action of the Rectus Femoris Muscle Following Distal Tendon Transfer: Does It Generate Knee Flexion Moment?," Dev. Med. Child Neurol., **39**(2), pp. 99–105.
[14] Yamaguchi, G. T., and Zajac, F. E., 1989, "A Planar Model of the Knee Joint to Characterize the Knee Extensor Mechanism," J. Biomech., **22**(1), pp. 1–10.
[15] Lu, T. W., O'Connor, J. J., Taylor, S. J., and Walker, P. S., 1997, "Validation of a Lower Limb Model With In Vivo Femoral Forces Telemetered From Two Subjects," J. Biomech., **31**(1), pp. 63–69.
[16] O'Connor, J. J., Shercliff, T. L., Biden, E., and Goodfellow, J. W., 1989, "The Geometry of the Knee in the Sagittal Plane," Proc. Inst. Mech. Eng., Part H: J. Eng. Med., **203**(4), pp. 223–233.
[17] Jonkers, I., Spaepen, A., Papaioannou, G., and Stewart, C., 2002, "An EMG-Based, Muscle Driven Forward Simulation of Single Support Phase of Gait," J. Biomech., **35**(5), pp. 609–619.
[18] Stansfield, B. W., Nicol, A. C., Paul, J. P., Kelly, I. G., Graichen, F., and Bergmann, G., 2003, "Direct Comparison of Calculated Hip Joint Contact Forces With Those Measured Using Instrumented Implants. An Evaluation of a Three-Dimensional Mathematical Model of the Lower Limb," J. Biomech., **36**(7), pp. 929–936.
[19] Raikova, R. T., and Prilutsky, B. I., 2001, "Sensitivity of Predicted Muscle Forces to Parameters of the Optimization-Based Human Leg Model Revealed by Analytical and Numerical Analyses," J. Biomech., **34**(10), pp. 1243–1255.
[20] D'Lima, D. D., Townsend, C. P., Arms, S. W., Morris, B. A., and Colwell, C. W., Jr., 2005, "An Implantable Telemetry Device to Measure Intra-Articular Tibial Forces," J. Biomech., **38**(2), pp. 299–304.
[21] Bergmann, G., Graichen, F., Siraky, J., Jendrzynski, H., and Rohlmann, A., 1988, "Multichannel Strain Gauge Telemetry for Orthopaedic Implants," J. Biomech., **21**(2), pp. 169–176.
[22] Arnold, A. S., Salinas, S., Asakawa, D. J., and Delp, S. L., 2000, "Accuracy of Muscle Moment Arms Estimated From MRI-Based Musculoskeletal Models of the Lower Extremity," Comput. Aided Surg., **5**(2), pp. 108–119.
[23] Smith, D. K., Berquist, T. H., An, K. N., Robb, R. A., and Chao, E. Y., 1989, "Validation of Three-Dimensional Reconstructions of Knee Anatomy: CT vs MR Imaging," J. Comput. Assist. Tomogr., **13**(2), pp. 294–301.
[24] Fukunaga, T., Roy, R. R., Shellock, F. G., Hodgson, J. A., Day, M. K., Lee, P. L., Kwong-Fu, H., and Edgerton, V. R., 1992, "Physiological Cross-Sectional Area of Human Leg Muscles Based on Magnetic Resonance Imaging," J. Orthop. Res., **10**(6), pp. 926–934.
[25] Koo, T. K., Mak, A. F., and Hung, L. K., 2002, "In Vivo Determination of Subject-Specific Musculotendon Parameters: Applications to the Prime Elbow Flexors in Normal and Hemiparetic Subjects," Clin. Biomech. (Bristol, Avon), **17**(5), pp. 390–399.
[26] Reinbolt, J. A., Haftka, R. T., Chmielewski, T. L., and Fregly, B. J., 2007, "Are Patient-Specific Joint and Inertial Parameters Necessary for Accurate Inverse Dynamics Analyses of Gait?," IEEE Trans. Biomed. Eng., **54**(5), pp. 782–793.
[27] Scovil, C. Y., and Ronsky, J. L., 2006, "Sensitivity of a Hill-Based Muscle Model to Perturbations in Model Parameters," J. Biomech., **39**(11), pp. 2055–2063.
[28] Neptune, R. R., and Hull, M. L., 1998, "Evaluation of Performance Criteria for Simulation of Submaximal Steady-State Cycling Using a Forward Dynamic Model," J. Biomech. Eng., **120**(3), pp. 334–341.
[29] Raasch, C. C., Zajac, F. E., Ma, B., and Levine, W. S., 1997, "Muscle Coordination of Maximum-Speed Pedaling," J. Biomech., **30**(6), pp. 595–602.
[30] Hakansson, N. A., and Hull, M. L., 2007, "Influence of Pedaling Rate on Muscle Mechanical Energy in Low Power Recumbent Pedaling Using Forward Dynamic Simulations," IEEE Trans. Neural Syst. Rehabil. Eng., **15**(4), pp. 509–516.
[31] Delp, S. L., and Loan, J. P., 2000, "A Computation Framework for Simulation and Analysis of Human and Animal Movement," IEEE Comput. Sci. Eng., **2**(5), pp. 46–55.
[32] Fregly, B. J., 1993, "The Significance of Crank Load Dynamics to Steadystate Pedaling Biomechanics: An Experimental and Computer Modeling Study," Ph.D. thesis, Stanford University, Palo Alto, CA.
[33] Thelen, D. G., Anderson, F. C., and Delp, S. L., 2003, "Generating Dynamic Simulations of Movement Using Computed Muscle Control," J. Biomech., **36**(3), pp. 321–328.
[34] Thelen, D. G., and Anderson, F. C., 2006, "Using Computed Muscle Control to Generate Forward Dynamic Simulations of Human Walking From Experimental Data," J. Biomech., **39**(6), pp. 1107–1115.
[35] Anderson, F. C., and Pandy, M. G., 2001, "Static and Dynamic Optimization Solutions for Gait are Practically Equivalent," J. Biomech., **34**(2), pp. 153–161.
[36] Hakansson, N. A., and Hull, M. L., 2005, "Functional Roles of the Leg Muscles When Pedaling in the Recumbent Versus the Upright Position," ASME J. Biomech. Eng., **127**(2), pp. 301–310.
[37] Koehle, M. J., and Hull, M. L., 2008, "A Method of Calculating Physiologically Relevant Joint Reaction Forces During Forward Dynamic Simulations of Movement From an Existing Knee Model," J. Biomech., **41**(5), pp. 1143–1146.
[38] Delp, S. L., Loan, J. P., Hoy, M. G., Zajac, F. E., Topp, E. L., and Rosen, J. M., 1990, "An Interactive Graphics-Based Model of the Lower Extremity to Study Orthopaedic Surgical Procedures," IEEE Trans. Biomed. Eng., **37**(8), pp. 757–767.
[39] Zavatsky, A. B., and O'Connor, J. J., 1992, "A Model of Human Knee Ligaments in the Sagittal Plane. Part 1: Response to Passive Flexion," Proc. Inst. Mech. Eng., Part H: J. Eng. Med., **206**(3), pp. 125–134.
[40] van Dijk, R., Huiskes, R., and Selvik, G., 1979, "Roentgen Stereophotogrammetric Methods for the Evaluation of the Three Dimensional Kinematic Behaviour and Cruciate Ligament Length Patterns of the Human Knee Joint," J. Biomech., **12**(9), pp. 727–731.
[41] Yoshioka, Y., Siu, D. W., Scudamore, R. A., and Cooke, T. D., 1989, "Tibial Anatomy and Functional Axes," J. Orthop. Res., **7**(1), pp. 132–137.
[42] Asano, T., Akagi, M., and Nakamura, T., 2005, "The Functional Flexion-Extension Axis of the Knee Corresponds to the Surgical Epicondylar Axis: In Vivo Analysis Using a Biplanar Image-Matching Technique," J. Arthroplasty, **20**(8), pp. 1060–1067.
[43] Mensch, J. S., and Amstutz, H. C., 1975, "Knee Morphology as a Guide to Knee Replacement," Clin. Orthop. Relat. Res., **112**, pp. 231–241.
[44] Koehle, M. J., 2007, "Development of Knee Models for Use in Forward Dynamic Simulations of Movement and Their Effect on Simulation Results," MS Thesis in Biomedical Engineering, University of California at Davis, Davis, CA.
[45] van Eijden, T. M., de Boer, W., and Weijs, W. A., 1985, "The Orientation of the Distal Part of the Quadriceps Femoris Muscle as a Function of the Knee Flexion-Extension Angle," J. Biomech., **18**(10), pp. 803–809.
[46] Gill, H. S., and O'Connor, J. J., 1996, "Biarticulating Two-Dimensional Computer Model of the Human Patellofemoral Joint," Clin Biomech. (Bristal, Avon), **11**(2), pp. 81–89.
[47] Montgomery, S. C., Moorehead, J. D., Davidson, J. S., Lowe, D., and Dangerfield, P. H., 1998, "A New Technique for Measuring the Rotational Axis Pathway of a Moving Knee," The Knee, **5**(4), pp. 289–295.